Journal of Nano- and Electronic Physics
Vol. **10** No 1, 01001(4pp) (2018)

Журнал нано- та електронної фізики
Том **10** № 1, 01001(4cc) (2018)

Effect of Sintering Temperature on Structural Properties of Cd doped Co-Zn Ferrite

Akshay B. Kulkarni[1], Shridhar N. Mathad[2,*]

[1] *Department of Physics, Jain College of Engineering, 590014 Belagavi, India*
[2] *K.L.E. Institute of Technology, 580030 Hubballi, India*

(Received 10 October 2017; revised manuscript received 25 November 2017; published online 24 February 2018)

This work has the objective of influence of sintering temperatures (800 °C and 1000 °C) structural properties of cadmium doped cobalt zinc ferrite ($Co_{0.5}Zn_{0.5}Cd_{0.2}Fe_{1.8}O_4$) prepared by simple, low-cost Solid State reaction method. The structural parameters were explored by XRD technique. The X-ray analysis confirms the formation of particles of cubic inverse spinel structure. The structural and mechanical properties comparatively reported.

Keywords: Cadmium doped cobalt zinc ferrites ($Co_{0.5}Zn_{0.5}Cd_{0.2}Fe_{1.8}O_4$), XRD, Texture coefficients, Crystallite size.

DOI: 10.21272/jnep.10(1).01001 PACS numbers: 75.50.Gg, 61.05.cp

1. INTRODUCTION

Ferrites (ferrimagnetic oxides) are dark brown or gray in appearance and very hard and brittle in physical character. They are groomed by heat-treating of the mixture of various transition metal oxides or alkaline earth oxides with the ferric oxides. Properties of ferrites depend upon the nature, oxidation state and distribution of metal ions over tetrahedral and octahedral sites. Ferrites have been potential candidate for technological and commercial applications in electric and magnetic fields. Spinel ferrites have been widely studied due to their interesting properties like high resistivity, mechanical hardness, remarkable stability and promising memory storage capacity [1-3].

Cobalt ferrite is an inverse spinel ferrite, whose degree of inversion relies on synthesis method. At room temperature, cobalt ferrite has been under study due to its very interesting features like high coercivity, good electrical insulation, high chemical stability and moderate saturation magnetization [4]. The cobalt ferrites behave like energy efficient actuators. The pursuit in these ferrites is intensifying due to strong magneto-elastic effect. Cobalt ferrites become a promising candidate for investigation as an alternative ceramic material for developing novel magnetostrictive smart materials, magneto-optical storing media and magnetic recording [4-6].

In rare earthed doped (liked Gd, Pr, Dy, Ho and Er) $CoFe_2O_4$ crystallites, grain size are reported and magnetic properties enhancement have been observed [5-6]. In Nickel substituted Co-Zn ferrites inversion of cations at both tetrahedral A and octahedral B sites is observed and saturation magnetization decreased with increase in annealing temperature as reported [7]. The effect of zinc [8] and manganese [5] substituted Co-Zn ferrites on crystallite size and magnetic properties explored. Fascinatingly the substitution of cadmium (Cd) ion into the spinel lattice has significant variation on magnetic properties such as spin canting impression. [9] Structural, electrical, optical and magnetic properties of Cadmium substituted cobalt-zinc nanoferrites prepared by sol-gel auto-combustion method [10]. These ferrites can be and processed by versatile techniques such as auto combustion method [10], co-precipitation method [11], aerosol method [12], and sucrose precursor sol-gel combustion [13] and solid state method [14] and microwave method [15].

In this paper synthesis and structural analysis of cadmium doped Co-Zn ferrites sintered at 800 °C and 1000 °C is presented, which are prepared by solid state method. The influence of sintering temperature on structural behavior of ferrites like change such lattice constant, average particle size, hopping length, ionic radii, and mechanical properties were reported.

2. EXPERIMENTAL

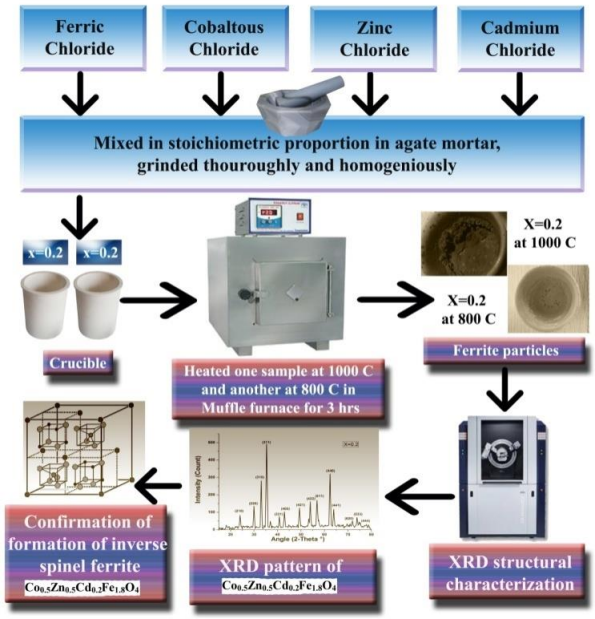

Fig. 1 – Schematic diagram of Solid State reaction method of $Co_{0.5}Zn_{0.5}Cd_{0.2}Fe_{1.8}O_4$ ferrite for 800 °C and 1000 °C sintering temperatures

*physicssiddu@gmail.com

All of the starting materials like $CdCl_2.H_2O$, $ZnCl_2$, $FeCl_3.6H_2O$ and $CoCl_2.6H_2O$ were analytical grade in stoichiometry, used to synthesis the ($Co_{0.5}Zn_{0.5}Cd_{0.2}Fe_{1.8}O_4$) by standard solid state reaction method (shown in Fig. 1). The mixture of chemicals were grind in the agate-mortar for 5 hour to get homogeneous finely powdered and heated in a muffle furnace in silica crucible sintered at 800 °C for 3 hours and at 1000 °C for 3 hours for another sample. Structural characterization of the ferrite powders was carried out X-ray Diffractometer, (with Cu-Kα radiation, wavelength, $\lambda = 1.5406$ Å).

$$CoCl_2.6H_2O + ZnCl_2 + FeCl_3.6H_2O + CdCl_2.H_2O \rightarrow Co_{0.5}Zn_{0.5}Cd_{0.2}Fe_{1.8}O_4 + nH_2O\uparrow + nCl_2\uparrow$$

3. RESULTS AND DISCUSSION

3.1 X-Ray Diffraction Studies

The peaks position and relative intensity matches with the standard $Co_{0.5}Zn_{0.5}Cd_{0.2}Fe_{1.8}O_4$ (JCPDC card #00-22-1086). This shows that synthesized sample belongs to cubic inverse spinel structure with lattice constant 8.4055 Å for sintering temperature 1000 °C and 8.3925 Å for sintering temperature 800 °C, Miller indices (HKL) and lattice parameter (a) were calculated and tabulated in Table 1.

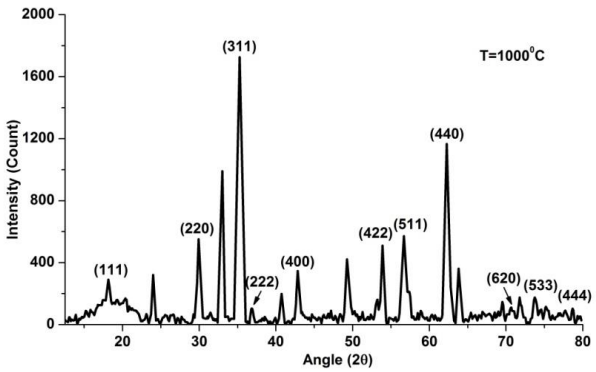

Fig. 2 – XRD pattern of $Co_{0.5}Zn_{0.5}Cd_{0.2}Fe_{1.8}O_4$-ferrite synthesized by Solid State reaction method sintered at 1000 °C

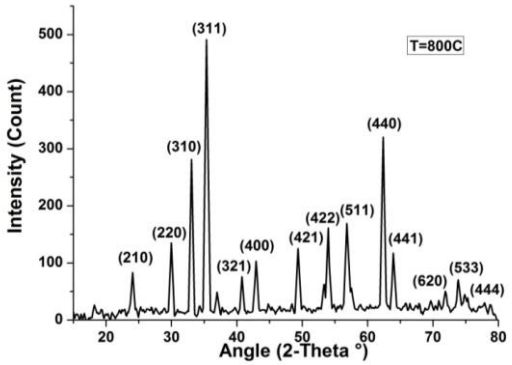

Fig. 3 – XRD pattern of $Co_{0.5}Zn_{0.5}Cd_{0.2}Fe_{1.8}O_4$-ferrite synthesized by Solid State reaction method sintered at 800 °C

Table 1 – Calculation of lattice parameter

	$X = 0.2$ at 1000 °C			$X = 0.2$ at 800 °C		
hkl	Angle 2θ	Observed Intensity %	Lattice parameter a (Å)	Angle 2θ	Observed Intensity %	Lattice parameter a (Å)
2 1 0	23.996	18.6	8.2858	24.041	16.9	8.2705
2 2 0	29.902	31.9	8.4448	29.967	27.5	8.4272
3 1 0	33.006	57.4	8.5751	33.056	57.2	8.5626
3 1 1	35.265	100	8.4341	35.367	100	8.4107
3 2 1	40.722	11.5	8.2838	40.772	15.4	8.2740
4 0 0	42.828	20.1	8.4393	42.944	20.9	8.4175
4 2 1	49.799	6.5	8.3841	49.362	25.6	8.4536
4 2 2	53.891	29.6	8.3277	53.971	32.8	8.3164
5 1 1	56.682	33.1	8.4315	56.827	34.5	8.4118
4 4 0	62.258	67.6	8.4290	62.376	65.3	8.4146
4 4 1	63.793	20.9	8.3747	63.924	23.9	8.3593
6 2 0	70.618	6.4	8.4289	70.905	7	8.3992
5 3 3	73.735	10.2	8.4191	73.865	14.3	8.4064
4 4 4	78.672	6	8.4194	78.723	5.4	8.4149
Lattice Parameter			8.4055			8.3925

$$2d_{hkl}\sin\theta = n\,\lambda \quad (1)$$

$$d = \frac{a}{(h^2+k^2+l^2)^{1/2}} \quad (2)$$

$$D = \frac{K\cdot\lambda}{\beta_D.\cos\theta} \quad (3)$$

$$L_A = \frac{a\times\sqrt{3}}{4} \quad (4)$$

$$L_B = \frac{a\times\sqrt{2}}{4} \quad (5)$$

$$A-O = (u-1/4)a\sqrt{3} \quad (6)$$

$$B-O = (5/8-u)a \quad (7)$$

$$r_A = (u - 1/4)a\sqrt{3} - r(O^{2-}) \quad (8)$$

$$r_B = (5/8 - u)a - r(O^{2-}) \quad (9)$$

$$a = \left[\frac{2\pi^2}{45\sqrt{3}}\right]\frac{[\Delta 2\theta]}{\tan\theta_{hkl}} \quad (10)$$

$$micro - strain(\varepsilon) = \frac{\beta\cos\theta}{4} \quad (11)$$

$$\text{Dislocation Density}\,(\rho_D) = \frac{1}{D^2} \quad (12)$$

The lattice parameter ($a = b = c$), cell volume (V), Dislocation density (ρ_D) and Hopping length for tetrahedral site (L_A) and octahedral site (L_B) of ferrite samples are tabulated in Table 2.

The bond lengths (A–O and B–O) and ionic radii (r_A and r_B) on A-site and B-site are calculated using the equation. The calculated values of bond lengths and ionic radii on A-site and B-site are presented in Table 2.

3.2 Williamson Hall Plot and Size-Strain Plot Method [16]

The broadening of peaks are additive components (β_S broadening due to imperfections and β_D broadening due to crystallite size), size and strain plot is dependent on integral breadth of the peak. The distinct θ dependencies of both effects are the basis of analysis of Williamson and Hall for size and strain broadening [16].

$$\beta_{hkl}\cos\theta = \frac{K\cdot\lambda}{D} + 4\varepsilon\sin\theta \quad (13)$$

The "size-strain plot" (SSP) is used to understand the isotropic nature and micro-strain contribution. The size-strain parameters calculated by SSP have the advantage that less weight is given to data from reflections at high angles, where the precision is usually lower.

$$(d_{hkl}\beta_{hkl}\cos\theta)^2 = \frac{K.\lambda}{D}(d_{hkl}^2\beta_{hkl}\cos\theta) + \left(\frac{\varepsilon}{2}\right)^2 \quad (14)$$

Where K is a constant that depends on the shape of the particles; for spherical particles it is given as 3/4. The term $(d_{hkl}\beta_{hkl}\cos\theta)^2$ is plotted with respect to $(d_{hkl}^2\beta_{hkl}\cos\theta)$. In this case, the correlation between W-H plot and SSP has been reported in Table 3.

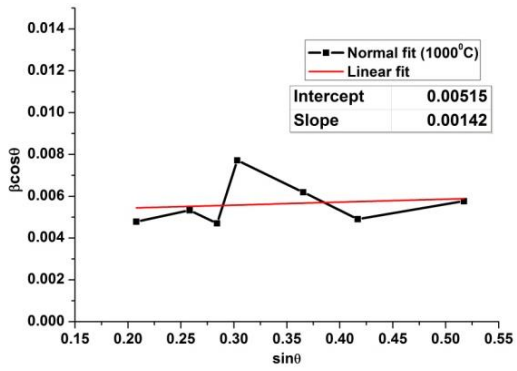

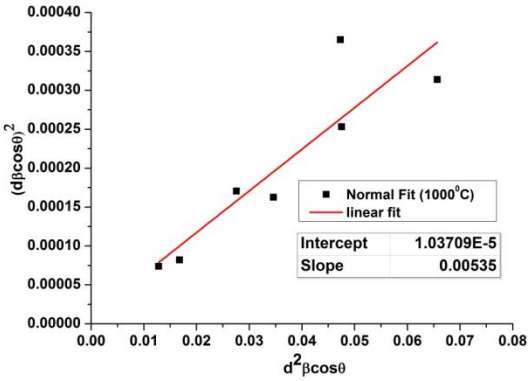

Fig. 4 – W-H graph of $\beta\cos\theta$ vs $\sin\theta$ and Size Strain plot $(d\beta\cos\theta)^2$ vs $d^2\beta\cos\theta$ for $Co_{0.5}Zn_{0.5}Cd_{0.2}Fe_{1.8}O_4$-ferrite at sintering temperature 1000 °C

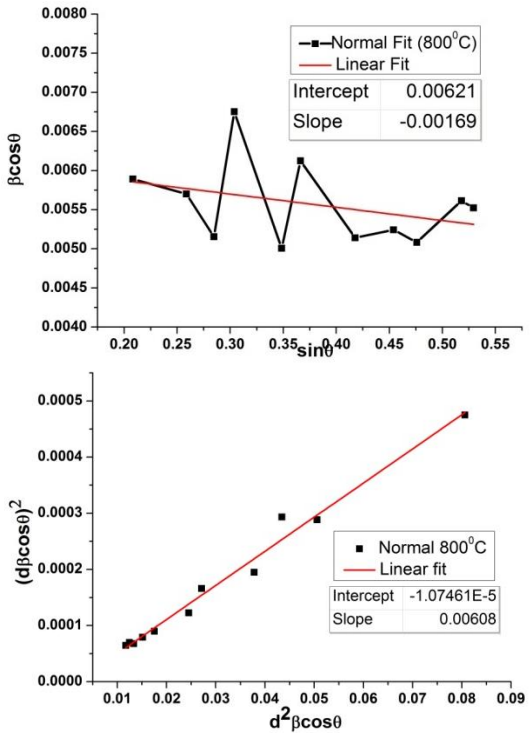

Fig. 5 – W-H graph of $\beta\cos\theta$ vs $\sin\theta$ and Size Strain plot $(d\beta\cos\theta)^2$ vs $d^2\beta\cos\theta$ for $Co_{0.5}Zn_{0.5}Cd_{0.2}Fe_{1.8}O_4$-ferrite at sintering temperature 1000 °C

3.3 Standard Deviation

The growth mechanism of ferrite sample can be estimated by calculating the standard deviation [16] using the equation

$$\sigma = \sqrt{\frac{\sum I_{hkl}^2 - (I_{hkl}^2/2)}{N}} \quad (15)$$

Where I_{hkl} stands for relative intensity of the (hkl) plane. The estimated standard deviation, σ, in the relative intensity values was calculated by taking the peak of hkl (220), (400), (422), (511) and (440) of five strongest indexed lines, excluding the line with $I_{hkl} = 100$. The calculated value of σ is 37.8029 for 1000 °C, and 37.2353 for 800 °C which seems to be showing almost same behavior that heterogeneous nucleation, desorption and adsorption are dominating.

Table 2 – Calculated values of lattice parameter (a), Volume of unit cell (V), X-ray Density Δx, Hopping length (L_A and L_B), Bond length (A-O and B-O), Ionic radii (r_A and r_B) and Staking fault probability

Temperature for $X = 0.2$	1000 °C	800 °C	Temperature for $X = 0.2$	1000 °C	800 °C
a (with all lines)	8.4055	8.3925	Bond Length A-O (Å)	1.8198	1.817
Crystallite size (Å)	253.06	250.99	Bond length A-B (Å)	2.1014	2.0981
Dislocation Density ρ_D	1.70E+15	1.63E+15	Ionic Radii r_A (Å)	0.4698	0.467
Micro Strain ε	0.001407	0.00139	Ionic Radii r_B (Å)	0.7514	0.7481
Volume of unit cell V (e^{-30})	593.87	591.12	x-ray density Δx (gr/cm^3)	5.5736	5.5995
Hopping length L_A (Å)	3.6397	3.6341	Standard Deviation	37.8029	37.2353
Hopping length L_B (Å)	2.9718	2.9672	Stalking fault coefficient α	0.00322	0.00324

Table 3 – Comparative values of crystallite size (D) and micro strain (ε)

	Crystallite size			Micro strain		
Temperature $X = 0.2$	From W-H graph	From SSP	From formula	Micro strain ε = slope/4 (WH)	Micro strain ε = 2*sqrt(slope) (SSP)	From formula $\varepsilon = \beta\cos\theta/4$
1000 °C	269.23	215.97	253.06	0.00035	0.00644	0.001407
800 °C	223.28	228.05	250.99	0.000423	0.006556	0.001392

4 Conclusions

The $Co_{0.5}Zn_{0.5}Cd_{0.2}Fe_{1.8}O_4$ successfully synthesized by Solid State reaction method at two different sintering temperatures of 1000 °C and 800 °C. The X-ray diffraction results for the samples of $Co_{0.5}Zn_{0.5}Cd_{0.2}Fe_{1.8}O_4$ showed the formation of single phase cubic spinel structure, having lattice constant and particle size 8.4055 Å and 8.3925 Å respectively. This shows the slight expansion of lattice unit cell with increase in temperature. The calculated particle size for 1000 °C is observed to be more compared to 800 °C; this is due to more particle agglomeration at higher temperature. In reverse the micro-strain observed to be decreasing with increase in temperature. The ionic radii, bond length and hopping lengths are observed to be increasing with increase in particle size (with increasing temperature). The Stalking fault coefficient (α) values for both sintering temperatures are very low which shows that all lines XRD pattern are matching with standard values and no anomalies observed. The dislocation density (ρ_D) and Standard Deviation (σ) of Cadmium doped Cobalt Zinc ferrite also reported.

REFERENCES

1. E.C. Snelling, *Soft Ferrites: Properties and Applications, 1st Edition* (Iliffe Books Ltd.: London: 1969).
2. A. Goldman, *Modern Ferrite Technology* (Springer-Verlag US: 2006).
3. A.J. Moulson, J.M. Herbert, *Electroceramics: Materials, Properties, Applications, 1st Edition* (Chapman & Hall: London: 1990).
4. H Cui, Y Jia, W Ren, W W J, *Sol-Gel Sci. Tecnol.* **55**, 36 (2010).
5. M. Atif, R. Sato Turtelli, R. Grössinger, M. Siddique, M. Nadeem, *Ceram. Int.* **40**, 471 (2014).
6. R.C. Kambale, K.M. Song, C.J. Won, K.D. Lee, N. Hur, *J. Cryst. Growth* **340**, 171 (2012).
7. O. Suwalka, R.K. Sharma, V. Sebastian, N. Lakshmi, K. Venugopalan, *J. Magn. Magn. Mater.* **313**, 198 (2007).
8. M. Mozaffari, S. Manouchehri, M.H. Yousefi, J. Amighian, *J. Magn. Magn. Mater.* **322**, 383 (2010).
9. S.S. Suryawanshi, V.V. Deshpande, U.B. Deshmukh, S.M. Kabur, N.D. Chaudhari, S.R. Sawant, *Mater. Chem. Phys.* **59**, 199 (1999).
10. S Bhukal, S Mor, S. Bansal, J Singh, S Singhal, *J. Molecular Structure* **1071**, 95 (2014).
11. S.S. Yattinahalli, S.B. Kapatkar, N.H. Ayachit, S.N. Mathad, *Int. J. Self-Propag. High Temp. Synth.* **22** No 3, 147 (2013).
12. S. Singhal, J Singh, S.K. Barthwal, K. Chandra, *J. Solid State Chem.* **178** No 10, 3183 (2005).
13. M.K. Rendale, S.N. Mathad, V. Puri, *Int. J. Self-Propag. High Temp. Synth.* **24** No 2, 78 (2015).
14. M.R. Patil, M.K. Rendale, S.N. Mathad, R.B. Pujar, *Int. J. Self-Propag. High Temp. Synth.* **24** No 4, 241 (2015).
15. A Molakeri, S Kalyane, A.B. Kulkarni, S.N. Mathad, *Int. J. Adv. Sci. Eng.* **3** No 4, 422 (2017).
16. A.K Zak, M.E. Abrishami, W.H.Abd. Majid, R Yousefi, S.M. Hosseini, *Ceram. Inter.* **37**, 393 (2011).